Determination of Binding Constant and Stoichiometry for Antibody-Antigen Interaction with Surface Plasmon Resonance

Shiming Lin[1,3,*], Adam Shih-Yuan Lee[2], Chih-Chen Lin[2] and Chih-Kung Lee[3]

[1]*Centre for Optoelectronic Biomedicine, National Taiwan University, Taipei, Taiwan;* [2]*Department of Chemistry, Tamkang University, Tamsui, Taiwan and* [3]*Institute of Applied Mechanics, National Taiwan University, Taipei, Taiwan*

Abstract: A surface plasmon resonance (SPR) biosensor technology has recently been applied biochemically and clinically to the study of immunologic recognition and the evaluation of binding parameters for various interactions between antibodies (Abs) and antigens (Ags) at liquid-solid interface. The simple interaction between hapten and Ab fragment, e.g., variable single-chain fragment and antigen-binding fragment, can be described sufficiently by a 1:1 stoichiometry in SPR. However, the determination of the binding constant of an anti-protein Ab is usually complicated by the multivalence of the protein Ag. The SPR-based method enables direct determination of binding constants for a variety of specific Ab-Ag interactions in real-time. It also allows estimation of the binding stoichiometry and binding ratio for low-, intermediate-, and high-affinity Ab-Ag interaction systems. The present review is designed to indicate the theoretical background of SPR-based biosensor technology as well as to present the great variety of measurement modes of interaction kinetics that can be performed with these techniques. Quantitative aspects of the Ab-Ag interaction kinetics are reviewed, focusing especially on mono- and multi-valent Ab-Ag interaction modes using a SPR biosensor. Four model binding systems developed recently for use with SPR biosenser are described with principles and examples: (i) one to one interaction mode, (ii) nonequivalent two-site interaction mode, (iii) multiple equivalent-site interaction mode and (iv) multisite interaction mode. This article closes with two descriptions of the determinations of the binding stoichiometry and maximum binding ratio of Ab-Ag interactions.

Key Words: Monoclonal antibody, variable single-chain fragment, antigen-binding fragment, binding constant, affinity, dissociation constant, dissociation rate constant, association rate constant, stoichiometry, maximum binding ratio, surface plasmon resonance, resonance unit.

1. INTRODUCTION

The experimental determination of the binding constant (affinity) of an antibody (Ab) for its antigen (Ag) is of considerable importance. This is the basic experimental parameter in a variety of studies, such as the use of Abs as conformational probes (Goldberg, 1991), or in a thermodynamic approach to the molecular basis of Ab-Ag interaction (Djavadi-Ohaniance and Friguet, 1992). Information obtained from binding stoichiometry allows one to measure the concentration of biologically active antigens (Fountoulakis *et al.*, 1992; Biemann and Koshland, 1994) and to predict the binding topology. Also, it might help to localize the binding sites (Okun *et al.*, 2001).

The single-chain antibody variable-region fragment (scFv), the smallest construction of an Ab that retains the complete binding site, and the antigen-binding fragment (Fab) from its monoclonal IgG preparation are monovalent and can combine with one haptenic Ag or with one separate epitope on the Ag molecule. The simplest case of Ab-Ag interaction is that of the interaction of scFv (or Fab) Ab with monovalent Ag, which includes truly monovalent haptenic Ag and a single, non-repeating site on the monomeric protein Ag. One molecule of immunoglobulin G (IgG) monoclonal antibody (mAb) has two identical combining sites and can combine with two separate homologous hapten molecules, with separate epitopes on two Ag molecules, or with two identical epitopes on one polymeric Ag molecule. Interactions between divalent mAb and monovalent Ag can be either cooperative or noncooperative: the binding at one site may or may not influence binding at another site. The monoclonal mAb preparation only contains one epitope specificity. However, the polyclonal Ab from immune serum contains a heterogeneous population of Abs which vary in concentration and in the strength (i.e., affinity) of their binding to the immunogen.

Based upon the Law of Mass Action, a variety of experimental approaches have been developed to facilitate the verification of an interaction and the calculations of binding parameters, such as the

dissociation constant, stoichiometry, and the kinetic constant for the interaction between di- or mono-valent Abs and mono- or multi-valent Ags (Berzofsky and Berkower, 1983). Among the various existing methods for estimating the binding parameters, most demand separation of free and bound reactants (e.g., equilibrium dialysis, ultracentrifugation, ultrafiltration, chromatography, and planar electrophoresis). They involve addition of reactants, mixing, incubation, and the subsequent determination of the concentration of the reactants or products at time intervals thereafter. Such conventional techniques, which have been widely used for the study of Ab-Ag interactions, can provide signals of individual interacting components (free Ab or Ag) and/or antibody-antigen complexes (AbAg), thus avoiding the disturbances caused by the matrix of coexisting compounds. However, they are constrained by a number of problems, such as loss of reactant due to non-specific adsorption, volume shift, inapplicability to unstable reactants due to time consumed, Donnan effect, leakage of bound reactants through membranes, deviation of Ab-Ag binding equilibrium, as well as estimation errors caused by viscosity, sedimentation, and back-diffusion (Liu *et al.*, 1999).

Surface plasmon resonance (SPR) biosensor technology has been established as a commercial instrument for almost 15 years. SPR-based BIAcore® instruments have recently been used to measure a variety of biomolecular interactions in real time (Jonsson, 1992). It is capable of characterizing binding reactions without labeling requirements. In a typical SPR experimental set-up, incident light is reflected from the internal face of a prism in which the external face has been coated with a thin metal film (Fig. **1**). At a critical angle, the intensity of the reflected light is lost to the creation of a resonant oscillation in the electrons at the surface of the metal film (Davies, 1994). Since the critical angle is dependent on the refractive index of the material present on the metal surface, this real-time method has been used to measure molecular interactions at solid-liquid interface. One reactant, referred to as the ligand, is immobilized to the sensor surface and the other reactant, referred to as the analyte, flows past this surface in solution. When the target and the probe interact to form a complex, a response is generated and monitored in real-time. SPR biosensors measure the change in refractive index in the vicinity of the surface of sensor chips to

*Address Correspondence to this author at the Center for Optoelectronic Biomedicine, National Taiwan University / College of Medicine, 1-1 Jen-Ai Road, Taipei 100, Taiwan; Fax: +886-2-23949125; E-mail: sml@ntumc.org

which ligands are immobilized (Markey, 1999). Because the changes in the refractive index are proportional to the changes in the adsorbed mass, the SPR technology allows detection of targets interacting with the probe immobilized on the sensor chip. It can thus be used to study the interactions of any biological system from proteins, oligosaccharides, oligonucleotides, and lipids to small molecules, viral particles, and bacterial cells. More fundamentally, the technique allows the direct observation of association and dissociation rate constants that contribute to the overall binding affinity (Lin *et al.*, 2005).
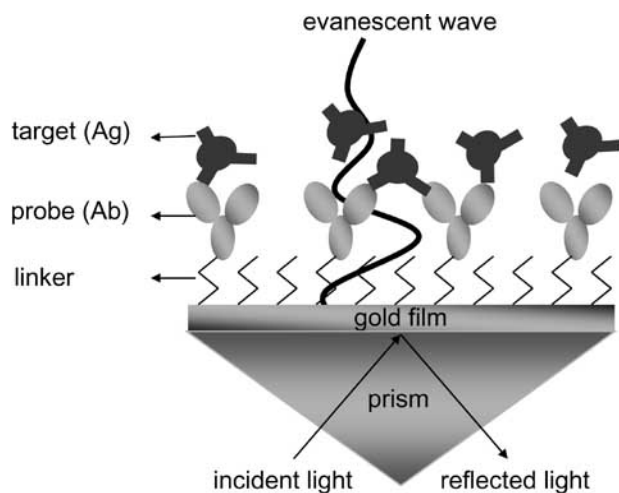

Fig. (1). In real-time biospecific interaction analysis, the binding events are detected using the optical phenomenon surface plasmon resonance, SPR. Under conditions of total internal reflection at a metal-coated interface, an evanescent wave propagates into the medium of low refractive index on the non-illuminated side. The SPR response is correlated to changes in refractive index at the sensor chip surface, caused by concentration changes on the sensor chip surface, e.g., when the target (Ag) binds to the immobilized probe (Ab). The SPR signal is monitored continuously so that interactions between target and probe can be studied in real time.
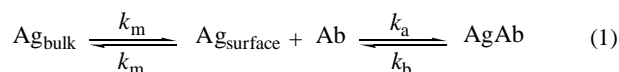
The use of SPR for the measurement of binding parameters for interactions has been reported. Qualitative applications range from follow up of purification (Lackmann *et al.*, 1996), epitope mapping (Myszka *et al.*, 1999), ligand fishing (Rich and Myszka, 2000) to identifying small molecule leads in a screening mode (Markgren *et al.*, 1999). Quantitative applications include measuring reaction kinetics (k_a, k_d) (Morton and Myszka, 1998) and binding constants (K_D) (Myszka *et al.*, 1998) and determining the active concentration of molecules (Zeder-Lutz *et al.*, 1999). Thermodynamic information can be obtained by measuring reaction rates and equilibrium constants at different temperatures (Roos *et al.*, 1998). When experiments are performed carefully, SPR biosensors can also be used to determine the binding stoichiometry and mechanism of the interaction (Morton and Myszka, 1998; Lin *et al.*, 2005).

The recent development of SPR-based biosensor technologies has made it possible to directly monitor the binding of low molecular mass compounds to immobilized macromolecules and thus allowed the study of fast molecular interaction kinetics and the evaluation of binding constants for Ab-Ag interactions in free solution (Table **1**). In these reports, the simpler Ab-Ag interaction can be sufficiently described by a 1:1 stoichiometry (Canziani *et al.*, 2004; Son *et al.*, 2004; Ja *et al.*, 2005; Dubreuil *et al.*, 2005). However, the determination of the binding constant for Ab-Ag interaction is complicated by the multivalence (multiple binding-sites) of the Ab (or Ag). When the Ab is monovalent, aggregates will not come up for a monovalent heptenic Ag. However, for (homo)polyvalent protein Ag (Gomes and Andreu, 2002; Herr *et al.*, 2003; Tobita *et al.*, 2004; Wittel *et al.* 2005; Yang *et al.*, 2005); aggre-

gates can be formed depending on conditions. The problem of aggregation can be minimized by the use of a very low concentration of reactants or by performing the determination with an analyte in excess. In addition, in some situations, the Ab (e.g., IgG and IgM) has two or multiple binding sites, each of which has a similar or different intrinsic affinity for binding independently to each Ag molecule (Herr *et al.*, 2003; Tobita *et al.*, 2004). It is not always easy to determine each of the intrinsic affinity. The problem of the heterogeneity of affinity of multivalent Ab (or Ag) still remains an obstacle to meaningful interpretation of data obtained. The objective of the present review is to be a tutorial with up to date examples to illustrate. It starts with the one to one interaction analysis of Ab-Ag interaction kinetics by SPR biosensor and follows with an in-depth description about the quantitative expression and evaluation of binding constants for Ab-Ag interaction kinetics by SPR method, with particular emphasis on the non-cooperativity and cooperativity of one, two, and poly binding sites on the related Ab (or Ag).

2. PRINCIPLE OF REAL-TIME Ab-Ag INTERACTION KINETICS

In SPR biosensors, one of the reactants, e.g., Ab (probe), is immobilized on a sensor chip. The other reactant, Ag (target), enters at one end, is transported by diffusion and flow to the sensor surface, where it reacts with immobilized Ab (Fig. **2A**). Change in the resonance signal expressed as resonance units (RU) are followed as a function of time and presented as a sensorgram (Fig. **2B**). From this data binding kinetics of the Ab-Ag interaction can be determined. The formation of surface-bound complex AgAb in the flow cell between target Ag and surface-bound probe Ab can be represented by the scheme

$$\text{Ag}_{\text{bulk}} \underset{k_m}{\overset{k_m}{\rightleftharpoons}} \text{Ag}_{\text{surface}} + \text{Ab} \underset{k_b}{\overset{k_a}{\rightleftharpoons}} \text{AgAb} \qquad (1)$$

where k_m is the rate constant for mass transport to and from the surface (the rate constant for mass transport is the same in both directions) and k_a and k_d are the association and dissociation rate constant for the formation of AgAb complex, respectively.

In the ideal situation, neither the transport of Ag to the sensor surface nor its transport within the linker layer influences the binding kinetics. This happens when transport is fast compared to binding. In this case the Ag concentration rapidly becomes uniform in space and constant in time, equals to the injection concentration $[B]_o$ in the bulk phase, and the measured forward and backward rate constants approximate to the constants for interaction kinetics (Glaser, 1993). Under these conditions, the rate of complex formation may be described as:

$$\text{d[AgAb]}/\text{d}t = k_a[\text{Ag}]([\text{Ab}]_o - [\text{AgAb}]) - k_d[\text{AgAb}] \qquad (2)$$

where [AgAb] is the amount of bound analyte, [Ag] is the amount of free Ag, $[\text{Ab}]_o$ is the total amount of Ab on the sensor surface. The on and off rates of binding are directly observable and the binding constants may be calculated by two methods described below.

2.1. Equilibrium Analysis

If the total amount of probe $[B]_o$ is expressed in terms of the maximum target binding capacity of the surface, i.e., the total amount of Ab binding-site on the sensor surface, all concentration terms can then be expressed as SPR response signal R, eliminating the need to convert from mass to molar concentration. Under pseudo first order conditions where the free target concentration is held constant in the flow cell, the binding can be described by Eq. [3]:

$$\text{d}R/\text{d}t = k_a C (R_{\text{max}} - R) - k_d R \qquad (3)$$

Table 1. **SPR-Based Studies of Biospecific Interaction Analysis between Abs and Ags**

Target [a]	Probe [b]	K_a (M^{-1}s^{-1}) [c]	K_d (s^{-1}) [d]	K_D(M) [e]	n [f]	Ref.
IgG1-Fc sFcγRIIb	sFcγRIIb IgG1-Fc Intact IgG1 R/A IgG1			$(0.98\pm0.01) \times 10^{-6}$ $(0.94\pm0.06) \times 10^{-6}$ $(0.95\pm0.02) \times 10^{-6}$ $(1.89\pm0.40) \times 10^{-6}$	1.00±0.04 0.91±0.01 0.97±0.04 1.06±0.02	[Mimura *et al.*, 2001]
Platelet-derived growth factor-BB (PDGF-BB)	basic fibroblast growth factor (bFGF)	$(1.27\pm0.06) \times 10^{6}$	$(1.71\pm0.06) \times 10^{-2}$	$(13.5\pm8.0) \times 10^{-9}$		[Russo *et al.*, 2002]
C-propeptide domains of procollagens (CRI) CRIII	Procollagen C-Proteinase enhancer (PCPE)			$(1.69\pm0.23) \times 10^{-7}$ $(3.69\pm0.5) \times 10^{-7}$	1 1	[Ricard-Blum *et al.*, 2002]
IgG1, κ (33D5) (37E1) IgG2a, λ (141D4)	StO4-BSA	1.8×10^{5} 2.3×10^{5} 1.2×10^{6}	1.0×10^{-4} 1.9×10^{-4} 3.9×10^{-4}	5.7×10^{-10} 8.0×10^{-10} 3.3×10^{-10}		[Leickt *et al.*, 2002]
FMDV antigenic peptide (152 nM) (305 nM) (610 nM) (1220 nM) (2440 nM)	anti-FMDV mAb	6.0×10^{4} 5.8×10^{4} 5.9×10^{4} 6.1×10^{4} 6.2×10^{4}	2.4×10^{-3} 2.6×10^{-3} 2.6×10^{-3} 2.7×10^{-3} 2.9×10^{-3}	4.0×10^{-8} 4.3×10^{-8} 4.3×10^{-8} 4.3×10^{-8} 4.8×10^{-8}		[Gomes and Andreu, 2002]
wild-type antigen of LFA-1 locked open mutant antigen of LFA-1	HI111 mAb	1.25×10^{5} 2.32×10^{4}	9.61×10^{-3} 9.72×10^{-3}	7.68×10^{-8} 4.19×10^{-7}		[Ma *et al.*, 2002]
murine-mAb (BIWA-1) (U36) chimeric-mAb (BIWA-2) humanized-mAb (BIWA-4) (BIWA-8)	GST/CD44v3-v10	1.3×10^{5} 1.5×10^{4} 1.7×10^{5} 6.5×10^{4} 7.5×10^{4}	4.2×10^{-5} 1.7×10^{-4} 4.1×10^{-5} 2.2×10^{-4} 6.3×10^{-5}	3.2×10^{-10} 1.1×10^{-8} 2.4×10^{-10} 3.4×10^{-9} 8.4×10^{-10}		[Verel *et al.*, 2002]
FcαRI Fcα	Fcα FcαRI	2.2×10^{5} (k_a1) 1.4×10^{5} (k_a2) 8.4×10^{4} (k_a1) 2.2×10^{4} (k_a2)	3.7×10^{-2} (k_d1) 6.8×10^{-2} (k_d2) 1.5×10^{-2} (k_d1) 2.0×10^{-3} (k_d2)	$169 \pm 10 \times 10^{-9}$ (K_D1) $494 \pm 101 \times 10^{-9}$ (K_D2) 180×10^{-9} (K_D1) 1170×10^{-9} (K_D2)		[Herr *et al.*, 2003]
anti-NP Fab (9T7) (9T8) (9T10) (9T13)	NP$_2$-HEL	5.5×10^{5} 5.4×10^{5} 1.8×10^{5} 3.9×10^{5}	1.3×10^{-2} 7.5×10^{-3} 2.3×10^{-3} 2.5×10^{-3}	2.4×10^{-8} 1.4×10^{-8} 1.3×10^{-8} 6.4×10^{-8}		[Sagawa *et al.*, 2003]
mAb (mAb11) (mAb5) (mAb12)	bovine cardiac troponin I (cTnI)	1.15×10^{4} 8.21×10^{3} 1.40×10^{3}	5.88×10^{-3} 5.49×10^{-3} 6.10×10^{-3}	5.10×10^{-7} 6.71×10^{-7} 4.35×10^{-6}	1 1 1	[Liu *et al.*, 2003]
NP$_{4.4}$-BSA NP$_{18.6}$-BSA NP$_{36.2}$-CGG NP$_{9.0}$-MMG NP$_{31.5}$-MMG NP$_{56.5}$-MMG NP$_{159}$-MMG	anti-NP IgG1 (A6-hCμ)			2.13×10^{-8} 1.52×10^{-9} 1.14×10^{-9} 7.69×10^{-9} 2.27×10^{-9} 1.96×10^{-9} 1.21×10^{-9}	0.59 0.71 0.40 0.14 0.15 0.14 0.16	[Tobita *et al.*, 2003]
hybridoma supernatant (H3) (A1) (B1) (C1) (D1) (B2)	Fc-specific IgG	$3.90[1]^g \times 10^{5}$ $4.54[3] \times 10^{5}$ $3.79[3] \times 10^{5}$ $4.37[5] \times 10^{5}$ $4.12[3] \times 10^{5}$ $2.18[4] \times 10^{5}$	$1.5[1]^h \times 10^{-4}$ $2.1[1] \times 10^{-4}$ $4.0[1] \times 10^{-4}$ $4.5[1] \times 10^{-4}$ $7.5[1] \times 10^{-4}$ $2.4[1] \times 10^{-4}$	$0.39[2]^i$ $0.45[1]$ $1.06[3]$ $1.04[2]$ $1.82[2]$ $1.10[4]$		[Canziani *et al.*, 2003]
mouse-mAb (BBK-4) humanized scFv (A12-1) (D4-2) (E4-1) (A-E5) (B-A5) (B-G2)	human 4-1BB receptor	1.25×10^{3} 4.18×10^{4} 1.29×10^{3} 1.72×10^{2} 5.07×10^{2} 4.51×10^{2} 2.32×10^{2}	5.88×10^{-7} 7.62×10^{-4} 8.35×10^{-6} 6.42×10^{-6} 9.39×10^{-6} 1.07×10^{-5} 1.16×10^{-5}	4.70×10^{-10} 1.82×10^{-8} 6.47×10^{-9} 3.73×10^{-8} 1.85×10^{-8} 2.38×10^{-8} 4.99×10^{-8}		[Son *et al.*, 2004]
a monomeric protein (Ag-1, MW 47 kDa) a monomeric polypeptide (Ag-2, MW 9.4 kDa) (Ag-2', MW 4.1 kDa)	mAb-1 mAb-2 mAb-2'	$4.6(0.1) \times 10^{5}$ $6.6(1.5) \times 10^{5}$ $2.7(0.6) \times 10^{6}$	$1.2(0.1) \times 10^{-3}$ $2.1(0.5) \times 10^{-5}$ $1.6(0.2) \times 10^{-5}$	$2.5(0.5) \times 10^{-9}$ $3.3(1.1) \times 10^{-11}$ $6.2(0.8) \times 10^{-12}$		[Drake *et al.*, 2004]
anti-Le^y antibody (hu3S193) (hu3S193-CalichDMH)	Le^y-BSA	8.3×10^{4} 3.7×10^{4}	1.0×10^{-3} 3.3×10^{-3}	1.3×10^{-8} 8.9×10^{-8}		[Boghaert *et al.*, 2004]
linear peptide 12p1 (RINNIPWSEAMM)	HIV envelope glycoprotein (YU2 gp120)			3.65×10^{-6}	1	[Biorn *et al.*, 2004]
anti-mAb (X1BRCTb)	mAb (L3BRCT)	1.31×10^{4}		1.02×10^{-9}		[Beernink *et al.*, 2005]

(Table 1) contd….

Target a	Probe b	Ka (M-1s-1) c	Kd (s-1) d	KD(M) e	n f	Ref.
human FcγRI (rsCD64)	hCG-cPIPP	1.7×10^6	1.8×10^{-4}	1.06×10^{-11}		[Paetz et al., 2005]
	ARP7073-2F5	1.5×10^6	3.8×10^{-4}	2.53×10^{-11}		
sc(Fv)₂	pancarcinoma tumor-associated antigen (TAG-72)			8.47×10^{-8}	2	[Wittel et al., 2005]
sc(Fv)₂-Ang II				1.19×10^{-7}	2	
HHHHHH-protein	Fab	7.3	23.82	3.26×10^{-6}		[Ja et al., 2005]
HHHHHH		9.9	5.78	5.80×10^{-7}		
HHHHHHHHHH		62.4	6.56	1.05×10^{-7}		
MDGHPERHDAGDHHHHHGVRQ		11.8	0.85	7.20×10^{-8}		
RHDAGDHHHHHGVRQ		21.5	0.82	3.80×10^{-8}		
MDGHPERHDAGDHHHHHGVRQWRLISTG-MBP		52.5	0.97	1.85×10^{-8}		
NSPGRFRHHHVLARRHALYR		17.4	0.27	1.55×10^{-8}		
MKVRRDVMRWHHHHRMARRKANR-MBP		40.9	0.31	7.60×10^{-9}		
scFv-His₆	Progesterone			$(0.020\pm0.009) \times 10^{-9}$	1	[Dubreuil et al., 2005]
	5β-DHP			$(0.028\pm0.009) \times 10^{-9}$	1	
	5α-DHP			$(0.097\pm0.028) \times 10^{-9}$	1	
interleukin-8 (IL-8)	mAb (MAB208)	1.46×10^6	2.06×10^{-6}	1.41×10^{-12}	1	[Yang et al., 2005]
	(JK8-2)	6.65×10^5	2.31×10^{-3}	3.48×10^{-9}	1	
human FcγRI (rsCD64)	human IgG	1.7×10^6	1.8×10^{-4}	1.1×10^{-10}	1	[Paetz et al., 2005]
HSA (pH 5.0)	shFcRn	$(14\pm2.5) \times 10^3$	$(5.8\pm0.3) \times 10^{-3}$	$(0.4\pm0.0) \times 10^{-6}$		[Chaudhury et al., 2006]
(pH 5.5)		$(9.3\pm0.0) \times 10^3$	$(6.9\pm0.6) \times 10^{-3}$	$(0.7\pm0.2) \times 10^{-6}$		
(pH 6.0)		$(7.7\pm1.1) \times 10^3$	$(8.5\pm3.0) \times 10^{-3}$	$(1.1\pm0.5) \times 10^{-6}$	1.1 ± 0.1	
(pH 6.5)		$(1.0\pm0.2) \times 10^3$	$(21.0\pm3.7) \times 10^{-3}$	$(21.6\pm5.8) \times 10^{-6}$		
(pH 7.0)		$(0.5\pm0.5) \times 10^3$	$(58.0\pm61) \times 10^{-3}$	$(116.6\pm63.6) \times 10^{-6}$		
shFcRn (pH 5.0)	HSA	$(35.9\pm4.1) \times 10^3$	$(6.3\pm0.7) \times 10^{-3}$	$(0.2\pm0.0) \times 10^{-6}$		
(pH 5.5)		$(27.0\pm2.6) \times 10^3$	$(7.8\pm0.4) \times 10^{-3}$	$(0.3\pm0.0) \times 10^{-6}$		
(pH 6.0)		$(16.6\pm1.5) \times 10^3$	$(15.2\pm0.4) \times 10^{-3}$	$(0.9\pm0.1) \times 10^{-6}$	1.1 ± 0.1	
(pH 6.5)		$(5.9\pm1.3) \times 10^3$	$(37.3\pm1.7) \times 10^{-3}$	$(6.5\pm1.1) \times 10^{-6}$		
(pH 7.0)		$(2.6\pm1.2) \times 10^3$	$(138\pm13.4) \times 10^{-3}$	$(72.8\pm60.3) \times 10^{-6}$		
hen egg white lysozyme (HEL)	anti-HEL mAb (HC1)	1.0×10^8	3.1×10^{-3}	3.10×10^{-11}	1.8	[Oda et al., 2006]
	(HC2)	1.5×10^8	2.7×10^{-3}	1.82×10^{-11}	2.1	
ovalbumin (OVA)	anti-OVA mAb (O1-1)	1.6×10^4	7.7×10^{-2}	4.81×10^{-6}	0.9	
	(YOVA)	3.9×10^4	3.5×10^{-4}	8.97×10^{-9}	1.0	
bovine serum albumin (BSA)	anti-BSA mAb (KM10)	1.5×10^5	4.5×10^{-4}	3.00×10^{-9}	1.1	
prostate-specific antigen (PSA)	anti-PSA mAb	$(4.1\pm0.6) \times 10^4$	$(4.5\pm0.6) \times 10^{-5}$	$(1.1\pm0.2) \times 10^{-9}$	1	[Katsamba et al., 2006]
scFv	Lewis x (Leˣ)			$(3.5\pm0.7) \times 10^{-5}$	1	[Johansson et al., 2006]
	sialyl Leˣ (sLeˣ)			$(2.6\pm0.7) \times 10^{-5}$	1	
scFv	murine laminin-1			9.9×10^{-8}	1	[Huang et al., 2006]
covalent diabody				4.4×10^{-10}	2	

where dR/dt is the rate of change of the SPR response signal, R and R_{max} are the measured and maximum response signal measured with binding, C is the injected concentration (M) of the Ag, k_a is the association rate constant or on-rate ($M^{-1}s^{-1}$) and k_d is the dissociation rate or off-rate (s^{-1}) (Fig. **3A**). The binding constant, i.e., association constants K_A, may be calculated as $K_A = k_a / k_d$ (M^{-1}). At equilibrium, $dR/dt = 0$ and Eq. [3] can be rewritten as:

$$R_{eq}/C = K_A R_{max} - K_A R_{eq} \qquad (4)$$

Therefore, the steady state association constant K_A can be obtained from a plot of R_{eq}/C versus R_{eq} and the dissociation constant K_D can be calculated as $1/K_A$ (Fig. **3B**).

2.2. Association Kinetics Analysis

Equation [3] may be rearranged as:

$$dR/dt = k_a C R_{max} - (k_a C + k_d)R \qquad (5)$$

Thus a plot of dR/dt against will theoretically be a straight line with slope $-(k_a C + k_d)$ for interaction-controlled kinetics. The initial binding rate (at R=0) is directly proportional to the analyte concentration and can be used for concentration measurements. If R_{max} is

known, both k_a and k_d can be determined from a single association sensorgram. R_{max} is however often difficult to determine experimentally, since a high analyte concentration is required to fully saturate the surface. A preferable approach is to measure the association sensorgram at several different analyte concentrations. For analysis of the on and off rates, a plot of the change in total detector response (dR/d_t) versus R gives a value S as the slope which relates the on and off rates as follows:

$$S = k_a C + k_d \qquad (6)$$

A plot of S against C will be a straight line with slope k_a (Fig. **3C**). In theory, the intercept on the ordinate ($C = 0$) give k_d: in practice, however, this cannot be used as a reliable measure of the dissociation rate constant if $k_a C \gg k_d$. A more accurate way to obtain this value is by direct measurement of the dissociation from saturated binding sites into a buffer solution flow that contains no Ag and the dissociation is quantified by:

$$\ln (R_o / R_t) = k_d (t - t_o) \qquad (7)$$

where R_o is the initial response level at t_o and R and t represent values obtained along the dissociation curve.
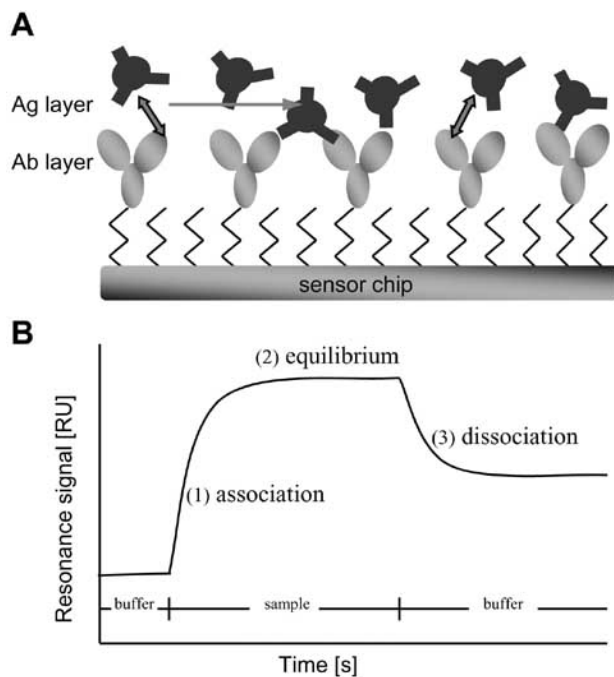
Fig. (2). (A) Schematic diagram depicting the interaction of Ag with Ab at liquid-solid interface. (B) Schematic sensorgram, showing association, equilibrium and dissociation phases. When Ag is injected in a discrete pulse across an Ab surface, the resulting sensorgram can be divided into three essential phases: (1) Association of Ag with Ab during sample injection; (2) Equilibrium or steady state during sample injection, where the rate of Ag binding is balanced by dissociation from the complex; (3) Dissociation of Ag from the surface during buffer flow. RU represents response unit.

3. ONE TO ONE INTERACTION MODE

3.1. Data Analysis

The theory of kinetic measurements for an Ag-Ab reaction analyzed in terms of the one to one interaction model has been described by Oda and Azuma (2000). The association rate constant, k_a, can be determined by carrying out a series of interaction experiments with different Ag concentration (C) and by measuring the binding rate, dR/dt, as a function of the SPR response (R) (Eq. [5]). Using linear transformation of the primary data, plots of dR/dt versus R are made for a range of Ag concentrations and the slopes of these curves, $S = k_aC + k_d$ (Eq. [6]), are determined. The S values are then plotted versus concentrations, and the new line obtained will have a slope corresponding to k_a. The dissociation rate constant, k_d, can be calculated from the dissociation phase described by Eq. [7]. A plot of ln (R_o/R_t) versus $t - t_o$ gives a straight line with slope k_d. The apparent binding (or association) constant, K_A, for the Ag-Ab interaction can then be determined as the ratio $K_A = k_a/k_d$ (or dissociation constant $K_D = k_d/k_a$).

3.2. Examples

3.2.1. Monovalent scfv – Monovalent Haptenic Ag Interaction

Dubreuil and co-workers (2005) investigated the binding of wild-type anti-progesterone (i) scFv$_{C12G11}$, (ii) mutant B14, and (iii) mutant B14 + Lys^{H31}-His^{H32} to soluble and unmodified progesterone, 5α- and 5β-dihydroprogesterone (DHP), respectively, by competition SPR experiments to develop a sensitive and highly specific *in vitro* immunoassay. The results obtained showed that mutant B14

+ Lys^{H31}-His^{H32} is much more specific than the wild-type antibody scFv fragment with deduced K_D values in the nanomolar range (5.3 and 2.4 x 10^{-9} M for 5α-DHP and 5β-DHP, respectively) *versus* 97 x 10^{-12} M (5α-DHP) and 28 x 10^{-12} M (5β-DHP) for the wild-type scFv fragment, whereas the affinity for progesterone remains in the picomolar range. Moreover, the improvement in specificity for their best mutant B14 + Lys^{H31}-His^{H32} compared with the wild-type scFv$_{C12G11}$ was calculated from measurement obtained under identical experimental conditions. It showed an increase in discrimination against 5α-DHP and 5β-DHP, 23-fold and 15-fold, respectively, compared with the starting scFv$_{C12G11}$ antibody. These improvements were calculated as cross-reaction percentages from experimentally measured K_D values. Furthermore, the lower cross-reactivity of mutant B14 + Lys^{H31}-His^{H32} was associated with a moderate 3.8- fold increase in the dissociation constant for progesterone (75 x 10^{-12} M *versus* 20 x 10^{-12} M).
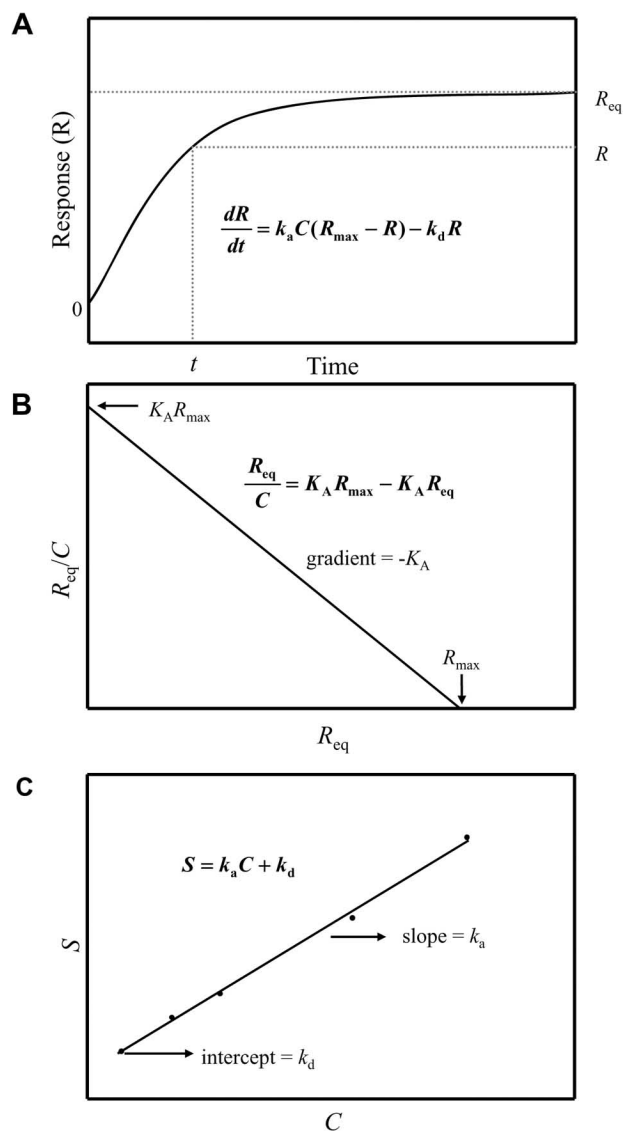

Fig. (3). (A) Simulated sensorgram illustrating affinity and kinetic measurement of Ag-Ab interaction according to Eq. [3]. (B) A plot of R_{eq}/C against R_{eq} at different Ag concentrations according to Eq. [4] thus gives a straight line from which R_{max} and K_A can be calculated. (C) A plot of slope value S versus Ag concentration C according to Eq. [6].

3.2.2. Monovalent scfv – Monomeric Protein Ag Interaction

Son and co-workers (2004) determined the kinetic constants for an interaction between human 4-1BB and soluble humanized scFv antibodies by SPR measurements. In this work, the humanization of agonistic anti-human 4-1BB mAb, BBK-4, using a phage display library, was presented. They prepared the combinatorial library by incorporating murine and human alternative at positions representing buried residues that might affect the structural integrity of the antigen binding site. Six humanized single chain Fv (scFv) fragments were selected from the combinatorial library expressing phage-displayed humanized scFv and found to retain the epitope specificity of the original mAb but had affinities of lower than 1/10 of the original. To obtain an association rate constant (k_a), the binding rate at five different humanized scFv concentrations ranging from 5 to 40 μg/ml in PBS was determined using SPR. Dissociation rate constants (k_d) were the average of five measurements obtained by analyzing the dissociation phase at an increased flow rate (40 μl/min). The dissociation constant (K_D) calculated from $K_D = k_d / k_a$ and was found to be (0.65~4.99) x 10^{-8}. These results suggest that humanized anti-human 4-1BB scFvs can be used as a valuable reagent for clinical application.

3.2.3. Monovalent Fab – Monovalent Haptenic Ag Interaction

Canziani *et al.*, (2004) determined kinetic parameters by SPR using the BIAcore biosensor system for the Ag–Ab interaction using a group of anti-(4-hydroxy-3-nitrophenyl)acetyl (NP) mAb whose differences in amino acid sequences had arisen only from somatic hypermutation. To investigate monovalent interaction, they prepared F_{ab} fragments of 9TX mAbs and passed them over the surface of the BIAcore SPR sensor chip, on which the NP-protein conjugates was immobilized. The kinetics of the binding of these F_{ab}s to the immobilized NP-hen egg white lysozyme (HEL) were essentially the same as to the immobilized NP-bovine serum albumin (BSA). The validity of the estimation of k_a (5.5 x 10^5 for 9T7Fab, 5.4 x 10^5 for 9T8, Fab 1.8 x 10^5 for 9T10 Fab, 3.9 x 10^5 for 9T13 Fab) or k_b (1.3 x 10^{-2} for 9T7Fab, 7.5 x 10^{-3} for 9T8, Fab 2.3 x 10^{-3} for 9T10 Fab, 2.5 x 10^{-3} for 9T13 Fab) was confirmed by the fact that the K_A values calculated from the two rate constants were similar to the $K_{A,eq}$ determined from Scatchard analysis. The kinetic analysis revealed that dissociation rates decreased during evolution. In addition, the k_a values of 9T7/9T8 were larger than those of 9T10/9T13. These results suggested that the mechanism for the Ag–Ab interaction shifted from a "zipper" type to a "lock-and-key" type during Ab evolution.

3.2.4 Monovalent Fab – Monovalent Peptide Ag Interaction

Ja and co-workers (2005) reported the interactions of anti-polyhistidine Fab with various peptides from the fragment selection synthesized or expressed for kinetic analysis by SPR technique. Absolute and relative binding constants obtained from mAb interactions with immobilized Ags are unreliable owing to the effects of rebinding and bivalency. To avoid these problems, Fab was prepared from anti-polyhistidine mAb and used as the analyte. Kinetic parameters were determined using a simple 1:1 bimolecular interaction model. The assayed peptides were categorized by their dissociation rates from the Fab, and the cited epitope, His_6, bound weakest to the Fab; the His_6 peptide and the His_6-tagged protein used in the original selection exhibited K_D values of 0.6 and 3 x 10^{-6} M, respectively. Additional His residues (His_{10} peptide) increased the association rate 6-fold without changing the dissociation rate significantly. In addition, kinetics measurements made by SPR, using purified Fab (antigen-binding fragment) to prevent avidity effects, demonstrated that the selected peptides bind with 10- to 75-fold higher affinities (K_D <75 x 10^{-9} M) than a hexahistidine peptide. The fragment library construction methodology described by the authors was applicable to the development of high-complexity protein or cDNA expression libraries for the identification of protein–protein interaction domains.

4. NONEQUIVALENT TWO-SITE INTERACTION MODE

4.1. Data Analysis

The SPR response (R) in the steady-state region is proportional to the amount of bound Ag. The maximum response per bound Ag (R_{max}) in the steady-state region can be predicted by Eq [8]:

$$R_{max} = R_{Ab} \times (MW\ Ag\ /\ MW\ Ab) \times RI \qquad (8)$$

where R_{Ab} is the amount of surface immobilized Ab in RUs, the second term on the right side of Eq [8] is the ratio of molecular weights of the Ag and Ab, and RI is the refractive index gradient ratio for the Ag and Ab. The RI values can be measured by using differential refractometry method (Mazur *et al.*, 2000).

Steady-state binding analysis is performed with multiple injections of different Ag concentrations over the immobilized Ab surface. Steady-state R values can be converted to r, where $r = R / R_{max}$, and the results can then be fit by nonlinear least squares methods to a two-site equilibrium model Eq. [9]:

$$r = (K_1C + 2K_1K_2C^2)\ /\ (1+K_1C + K_1K_2C^2) \qquad (9)$$

where r represents the moles of bound Ag per mole of Ab molecule, C is the unbound Ag concentration in equilibrium with the AgAb complex and is fixed by the concentration in the flow solution. K_1 and K_2 values are the macroscopic equilibrium constants for binding to the two sites.

4.2. Examples

Herr and co-workers (2003) investigated the binding mechanism for the interaction between a FcαRI, the receptor specific for the Fc region of IgA and a single Fcα homodimer by SPR experiments. Binding was monitored using both kinetic and equilibrium-based analysis. It was found that the kinetic data may be described by a bivalent ligand model in which two FcαRI molecules bind per dimeric Fcα molecule (Fig. **4**), consistent with the 2:1 stoichiometry observed by equilibrium gel-filtration analysis. The bivalent ligand model used to analyze the data included two sequential binding events, yielding two sets of apparent on-rate and off-rate constants ($k_a1 = 1.7$ x 10^5 M^{-1}s^{-1}, $k_d1 = 0.030$ s^{-1}, $k_a2 = 1.0$ x 10^5 M^{-1}s^{-1}, $k_d2 = 0.044$ s^{-1}). The derived or apparent rate constant for binding of the first molecule is equal to twice the intrinsic on-rate constant ($k_{a,app}1 = 2\ k_a1$); and the apparent rate constant for dissociation of the second molecule is equal to twice the intrinsic off-rate constant ($k_{d,app}2 = 2\ k_d2$). The intrinsic dissociation constants for binding of the first and second FcαRI molecule to Fcα were found to be similar ($K_D1 = 176$ nM; $K_D2 = 433$ nM) (Fig. **4A**), suggesting that receptor binding to one side of Fcα did not strongly influence the affinity of the second binding site, although there may be slight negative cooperativity. Comparable results were obtained by an equilibrium-based analysis of the binding data in which the data were globally fit to both one-site and two-site (bivalent ligand) models (Fig. **4B**).

5. MULTIPLE EQUIVALENT-SITE INTERACTION MODE

5.1. Data Analysis

When the observed response R values at high concentrations are greater than R_{max}, it points to more than one binding site in these Abs. The number of binding sites may be determined from Scatchard plots of R/C vs R plot (Eq. [4]) by a linear regression analysis. The R_{max} value is required to convert the observed response (R) to the standard binding parameter r (moles of Ag bound/moles of probe Ab), where $r = R / R_{max.}$ To obtain the binding constants, the results from the steady-state region are fitted with a multiple equivalent-site model, and Kaleidagraph is used for nonlinear least-squares optimization of the binding parameters (Carrasco *et al.*, 2002; Teulade-Fichou *et al.*, 2003) as follows:

$$r = nK_AC\ /\ (1 + K_AC) \qquad (10)$$

where K_A, the microscopic association constant, is one variable to fit; r represents the moles of bound Ag per mole of probe Ab; C is
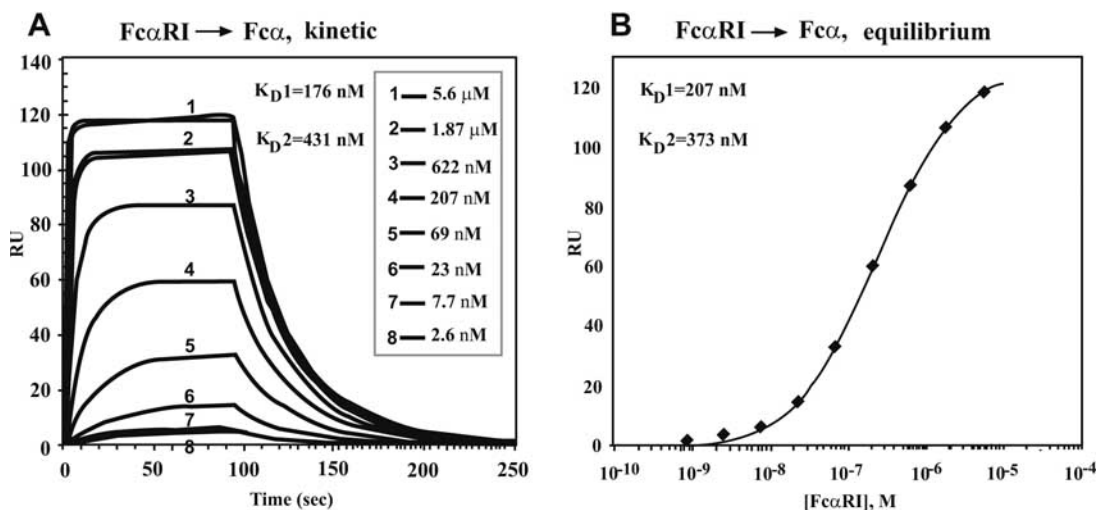
Fig. (4). Surface plasmon resonance analysis of the FcαRI:Fcα interaction. (A) Representative sensorgrams (colored lines) derived from injection of different concentrations of FcαRI over oriented coupled Fcα. Kinetic data were fitted globally using a bivalent ligand model (black lines). (B) Plot of equilibrium binding response (R_{eq}) *versus* concentration of injected analyte for the sensorgrams shown in (A). K_D was derived by global fitting of data from four experiments to a two-site binding model. A single representative curve is shown. Adapted with permission from Herr *et al.* (2003)**.**

the concentration of the Ag in equilibrium with the complex and is determined by the concentration in the flow solution; *n* is the number of equivalent Ag-binding sites on the Ab and is an integer larger than one (Fig. **5A**).

Equation [10] can be rearranged as follows:

$$r/C = K_A n - K_A r \tag{11}$$

Scatchard binding plot (*r/C* vs *r*) according to Eq. [11] is also usually used to determine the binding constant K_A and the number *n* of equivalent binding sites on the Ab (Fig. **5B**).
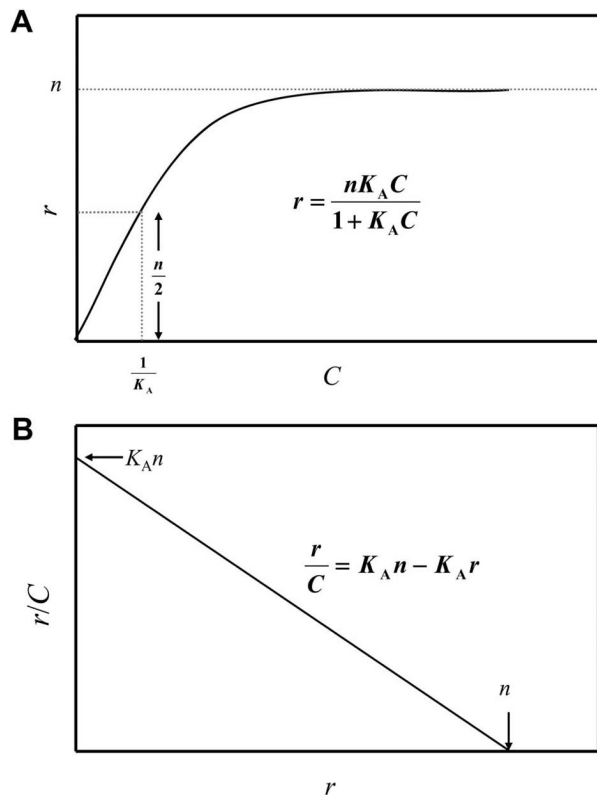
Fig. (5). (A) A binding curve of the number *r* of equivalent binding sites on the Ab versus Ag concentration *C* according to Eq. [10]. (B) Scatchard binding plot (*r/C* vs *r*) according to Eq. [11] thus gives a straight line from which *n* and K_A can be calculated.

5.2. Examples

5.2.1. Divalent scfv – Monomeric Protein Ag Interaction

Wittel and co-workers (2005) reported the interaction of pancarcinoma tumor-associated antigen 72 (TAG-72) with its antibody, a divalent single-chain Fv angiotensin II fusion construct of the monoclonal antibody (sc(Fv)$_2$-AngII). They engineered a dimeric sc(Fv)$_2$-AngII fusion construct that combines the superior kinetics of covalent dimeric scFvs [sc(Fv)$_2$], recognizing the TAG-72, with the advantageous intrinsic activity of AngII. SPR studies were performed to assess the off rates as well as the real-time binding kinetics of both constructs. As shown in Fig. **6**, the profiles obtained in the BIAcore evaluation of both constructs were similar. The on rates (k_{on}) were unaltered by the changes in the sc(Fv)$_2$-AngII molecule and were determined to be 2.97 x 10^4 and 2.84 x 10^4 (Ms)$^{-1}$ for sc(Fv)$_2$-AngII and sc(Fv)$_2$, respectively. Furthermore, the modifications of the sc(Fv)$_2$ did not lead to an alteration of the off rate (k_{off}), the rate an antibody diffuses off from its target molecule. The individual values obtained for the off rates were 2.52 x 10^{-3} s^{-1} for the sc(Fv)$_2$-AngII and 3.38 x 10^{-3} s^{-1} for the sc(Fv)$_2$. Consequently, the calculation of the kinetic association constants K_A did
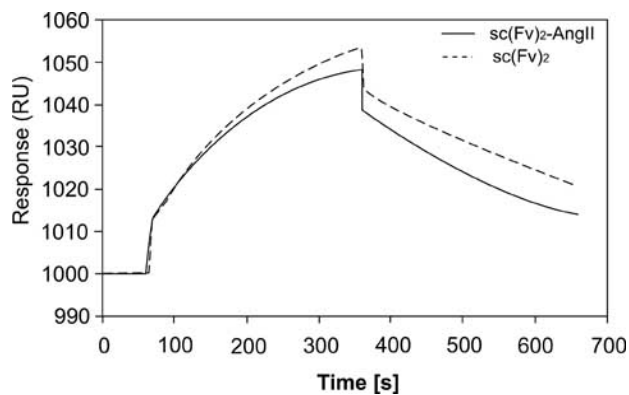

Fig. (6). Real-time binding kinetics of sc(Fv)$_2$ and sc(Fv)$_2$-AngII. The binding kinetics were analyzed by surface plasmon resonance to a bovine submaxillary gland mucin-coated chip. The two constructs exhibited similar on and off rates, and thus had comparable association constants, indicating that the altered design of sc(Fv)$_2$ had no effect on the inherent specific binding of the sc(Fv)$_2$. Reprinted with permission from Wittel *et al.* (2005)**.**

not reveal differences in the binding affinities of these two constructs and led to values of 1.18×10^7 M^{-1} for sc(Fv)$_2$-AngII and 8.42×10^6 M^{-1} for sc(Fv)$_2$, indicating that the altered design of sc(Fv)$_2$ had no effect on the inherent specific binding of the sc(Fv)$_2$.

5.2.2. Divalent mAb – Monovalent Haptenic Ag Interaction

Gomes and Andreu (2002) investigated the direct kinetic analysis of small antigenic peptides, foot-and-mouth disease viral (FMDV) peptides, interacting with immobilized anti-FMDV neutralizing mAb using SPR protocol. High peptide concentrations up to 2.5 μM and medium mAb surface densities about 1.5 ng/mm^2 were employed to ensure measurable binding levels, and fast buffer flow rates 60 μl/min were used to minimize diffusion-controlled kinetics. Good reproducibility levels in the kinetic constants were obtained under these analysis conditions (standard deviations below 10% of the mean values). The local fitting was performed using the separate k_a / k_d model and the locally fitted apparent rate constant, k_s, was plotted against peptide to check the linearity ($k_s = k_a \times C + k_d$). The locally fitted response at equilibrium, R_{eq}, was plotted against peptide concentration so that the affinity constant K_D values withdrawn from this plot could be calculated by the k_a / k_d ratio. Application of this protocol to determine the antigenic ranking of viral peptides showed an excellent agreement between SPR and previous competition enzyme-linked immunosorbent assays ELISA on the same peptide/antibody systems.

5.2.3. Divalent Mab –Monomeric Protein Ag Interaction

Yang and co-workers (2005) employed SPR biosensor technique to establish the first immunoassay for the quantification of picomolar interleukin-8 (IL-8) concentrations in human saliva in a microfluidic channel. They used a sandwich assay using two monoclonal antibodies (MAB208 and JK8-2), which recognize different epitopes on the antigen (IL-8). In order to measure picomolar concentrations of salivary IL-8, the kinetic parameters, dissociation constant (K_D), of the capture antibodies (MAB208 and JK8-2) were determined using SPR. A equivalent-site binding model was used that corrected for both linear baseline drift and bulk refractive index changes. The association rate constant (k_a) and dissociation rate constant (k_d) of MAB208 were 1.46×10^6 M^{-1} s^{-1} and 2.06×10^{-6} s^{-1}. The k_a and k_d of JK8-2 were 6.65×10^5 M^{-1} s^{-1} and 2.31×10^{-3} s^{-1}. The dissociation constants (K_D) of MAB208 and JK8-2 were 1.41 pM and 3.48 nM, respectively. The x2 value is a standard statistical measure of the closeness of fit. These kinetic measurements revealed that MAB208 had a higher affinity for IL-8 as well as a lower dissociation rate than JK8-2. Finallly, MAB208 was chosen as the primary capture (surface) antibody, and JK8-2 was chosen as the enhancing sandwich antibody for the quantification of picomolar concentrations of IL-8 in the saliva of healthy individuals and patients with oropharyngeal squamous cell carcinoma.

6. MULTISITE INTERACTION MODE

6.1. Data Analysis

The sensorgrams (resonance units, RU, vs time) are collected with the various concentration of samples injected. The RU values are averaged over a period of time span in the steady state response region and are converted to r (moles of Ag bound per mole of probe Ab) for binding analysis as previously described in section 4.1. The binding constants of the Ag to Ab are obtained from fitting a plot of r vs Ag concentration C. The plot is fitted with a one-, two-, three-, or four-site interaction model (for one-site model, $K_2 = K_3 = K_4 = 0$; for two-site model, $K_3 = K_4 = 0$; for three-site model, $K_4 = 0$) (Nguyen *et al.*, 2002):

$$r = (K_1 C + 2 K_1 K_2 C^2 + 3 K_1 K_2 K_3 C^3 + 4 K_1 K_2 K_3 K_4 C^4)/(1 + K_1 C + K_1 K_2 C^2 + K_1 K_2 K_3 C^3 + K_1 K_2 K_3 K_4 C^4) \quad (12)$$

6.2. Examples

Tobita and co-workers (2004) prepared IgG and IgM with identical combining sites to a hapten, (4-hydroxy-3-nitrophenyl) acetic acid (NP), and used SPR biosensor to evaluate the association constants (Ka) in interactions of these Abs with Ags which differed in the size of carriers and NP valence as well as in the stoichiometry of Ag to Ab in the immune complexes. It was found that IgM, a pentamer made up of five four-chain subunits and one J-chain, was unable to form an Ag$_1$Ab$_1$ complex with the highly haptenated Ag, NP18.6-BSA, such that one NP18.6-BSA molecule was held by multiple contacts with Fab arms from five subunits, although IgM was capable of forming an Ag$_4$Ab$_1$ complex in which each subunit was bound to one NP18.6-BSA molecule. It was also found that IgM was superior to IgG in interactions with large Ags of low hapten density. The Ka values of IgM to these Ags were estimated to be ~1×10^9 M^{-1}, about 20-fold higher than those of IgG. Reduction of inter-subunit and inter-chain disulfide bonds resulted in a decrease in Ka values to large Ags but no change in those to small Ags.

7. DETERMINATION OF STOICHIOMETRY

7.1. Data Analysis

The apparent stoichiometry of the surface complex (i.e. the number of Ag molecules that can bind to one Ab molecule) was calculated from the saturating binding capacity of the surface by the equation (Tobita *et al.*, 2004; Oda *et al.*, 2006):

$$\text{stoichiometry n} = \frac{R_{Ag}}{R_{Ab}} \times \frac{\text{MW Ab}}{\text{MW Ag}} = \frac{\text{RU}_{max} - \text{RU}_i}{\text{RU}_i - \text{RU}_0} \times \frac{\text{MW Ab}}{\text{MW Ag}} \quad (13)$$

where R_{Ab} is the SPR response of surface immobilized Ab in RUs. R_{Ag} is the observed response of bound antigen. Relationship between bound Ag ($\text{RU}_{max} - \text{RU}_i$) and amount of Ab ($\text{RU}_i - \text{RU}_o$) present on the sensor surface is displayed in (Fig. 7).
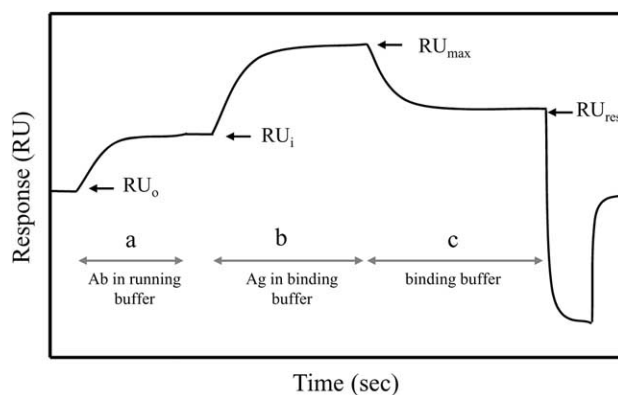

Fig. (7). A simple simulated sensorgram illustrating the binding of an Ag to an Ab immobilized on a sensor chip. A running buffer solution is pumped at a constant flow rate over the sensor surface. The sensorgram shows that injection of Ab generates an increase in the response expressed as resonance units (RU) (RU_i-RU_o) as shown in a. A pulse of sample containing the Ag is then injected and association of the Ag to the Ab is shown in b. An increase (RU_{max}-RU_i) of resonance unit is observed following an injection of a sample. The decrease of RU during the washing step (injection of binding buffer) is shown in c.

7.2. Example

Oda and co-workers (2006) investigated the interaction of Abs with protein Ags of different size, such as HEL, ovalbumin (OVA), and BSA, using SPR in order to estimate regional and segmental Ab flexibility. When Abs were immobilized on the surface of a sensor chip through the Fc region, the stoichiometry of the Ag–Ab complex was dependent on the Ag size; Ag$_2$Ab$_1$ forming with HEL and Ag$_1$Ab$_1$ with OVA and BSA. Typical sensorgrams for the bind-
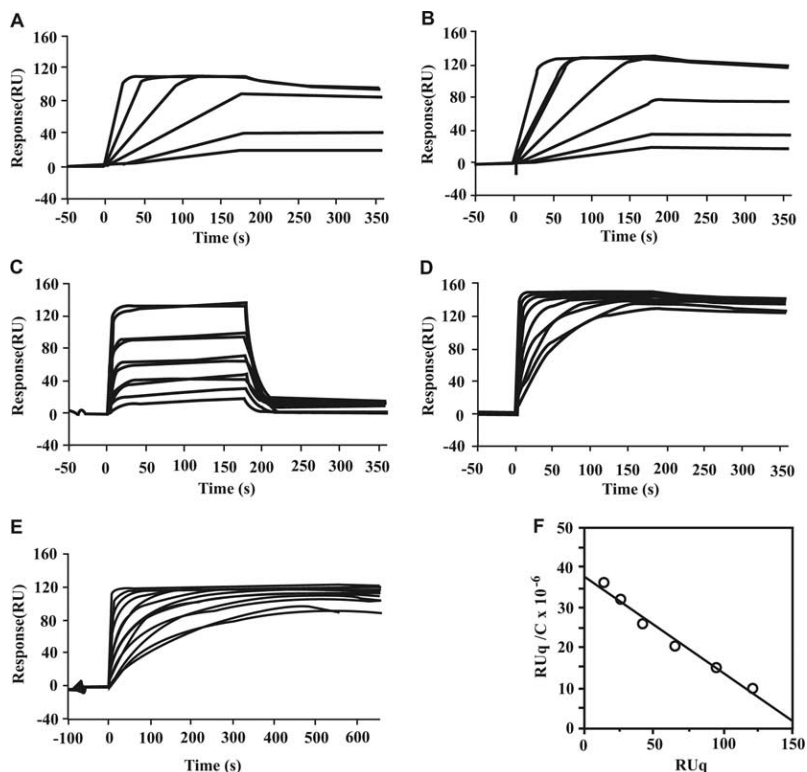
Fig. (8). SPR analysis of interactions between Ags and immobilized mAbs. (A–E) Sensorgrams for the interactions between HEL and HC1 anti-HEL mAb (A), between HEL and HC2 anti-HEL mAb (B), between OVA and O1-1 anti-OVA mAb (C), between OVA and YOVA anti-OVA mAb (D), and between BSA and KM10 anti-BSA mAb (E). Measurements were made at a concentration range of 0.78–25 nM for HEL, 400–12 800 nM for OVA, and 25–1600 nM for BSA. Sensorgrams (solid black lines) were subjected to nonlinear fitting (dotted grey line) to estimate the k_a and k_d values. The amounts of mAb immobilized by RAMFc Ab on the CM5 sensor chip were 650 RU of HC1, 650 RU of HC2, 608 RU of O1-1, 490 RU of YOVA, and 243 RU of KM10, respectively. (F) Scatchard plots for OVA binding to immobilized O1-1 anti-OVA mAb at a concentration of 400–12 800 nM. Adapted with permission from reference (Oda *et al.*, 2006).

ing of the Ag to the immobilized mAbs on the CM5 chip were shown in Fig. **8A-E**. In the case of OVA and O1-1, the interaction was evaluated using Scatchard plot analysis (Fig. **8F**), because the reaction proceeded rapidly and attained equilibrium within the measurement time. The plot was linear with a Ka value of 2.4 x 10^5 M^{-1}. Binding stoichiometries for the respective Ag–mAb interactions were 1.8 for HC1 anti-HEL mAb, 2.1 for HC2 anti-HEL mAb,

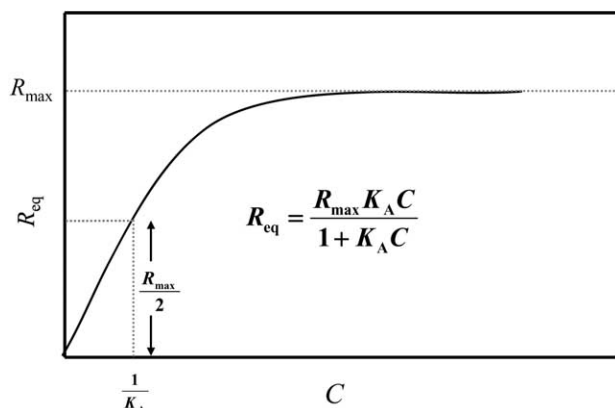**Fig. (9)**. A binding curve of the steady state binding response R_{eq} versus Ag concentration C according to Eq. [15].

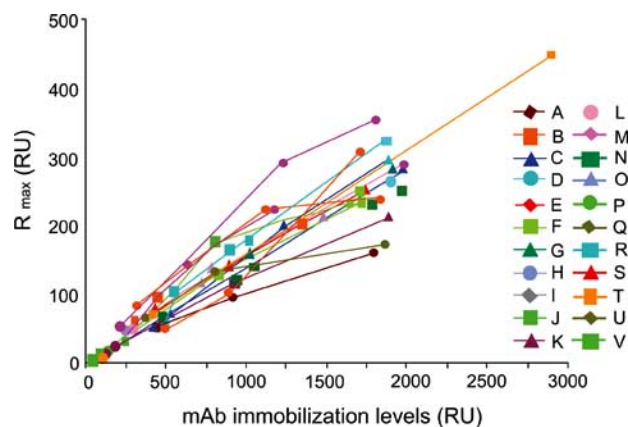$$R_{eq} = \frac{R_{max} K_A C}{1 + K_A C}$$

Fig. (10). Relationship between R_{max} and mAb immobilization levels R_{Ab}. The R_{max} calculated for each data set was plotted against the levels of mAb immobilized on multiple surfaces by the 22 participants (A-V). Reprinted with permission from reference (Katsamba *et al.*, 2006).

0.9 for O1-1 anti-OVA mAb, 1.0 for YOVA anti-OVA mAb and 1.1 for KM10 anti-BSA mAb. The results clearly show that an anti-HEL mAb can bind two HEL molecules simultaneously, whereas

anti-OVA or anti-BSA mAbs can bind only a single molecule of OVA or BSA, respectively. The results obtained allowed them to propose that the Fab arms of B-cell receptors whose Fc regions are immobilized on cell surface have a reduced dynamic range.

8. DETERMINATION OF MAXIMUM BINDING RATIO

8.1. Data Analysis

The measured SPR response in resonance units (RUs) is assumed to correlate to the surface concentration of immobilized Ab and Ag bound using the estimate 1 RU $\approx$ 1 pg mm^{-2} as has been done in the past for proteins (Yang *et al.*, 2005). Because of this, the maximum binding capacity or R_{max} value can be used to calculate a maximum binding ratio (mol Ag bound/mol Ab immobilized), assuming one set of independent noninteracting binding sites, using the following equation:

$$\text{maximum binding ratio} = \frac{R_{max}}{R_{Ab}} \times \frac{\text{MW Ab}}{\text{MW Ag}} \times \frac{1}{n} \qquad (14)$$

where R_{Ab} is the amount of surface immobilized Ab in RUs and n is the number of binding sites on the Ab. R_{max} is the maximum response at saturation of surface binding sites and can be determined by the method described below.

At equilibrium, dR/dt = 0 and Eq. [3] can be rearranged as follows:

$$R_{eq} = (R_{max}K_A C) / (1 + K_A C) \qquad (15)$$

where C is the concentration of Ag injected, K_A is the apparent association constant. R_{eq} is the measured response at equilibrium, and values of R_{eq} are obtained at a series of injected analyte C solution concentrations. The steady state response can be plotted versus the analyte concentration and the data are fit to a simple Langmuir isotherm for molecular interactions (Fig. **9**). R_{max} can then be calculated from the best fit of the binding curve.

Thus, the maximum binding ratio (Ag molecules per Ab) can be calculated by Eq. [14] using the R_{max} obtained by Eq. [15] and the known amount of Ab immobilized.

8.2. Examples

Katsamba and co-workers (2006) measured the binding of prostate-specific antigen (PSA) to a monoclonal anti-PSA antibody (mAb) to explore the reliability of Biacore-based SPR immunosensing. The mAb was immobilized on the sensor chip at three different densities and a two-step assay was used to determine the kinetic and affinity parameters of the PSA/mAb complex. The association and the extended-dissociation data derived from the three antibody surfaces were globally fitted using a simple 1:1 interaction model. The average k_a and k_d for the PSA/mAb interaction as calculated from the 22 analyses were $(4.1 \pm 0.6) \times 10^4$ M^{-1} s^{-1} and $(4.5 \pm 0.6) \times 10^{-5}$ s^{-1}, respectively. Based on the kinetic rate constants, the affinity (K_D) of the PSA/mAb interaction was 1.1 ± 0.2 nM. Fig. (**10**) shows the mAb immobilization level plotted against the R_{max} obtained from fitting the antigen binding response. As expected, this plot shows a nearly linear correlation between the level of mAb immobilized and the R_{max}. As the amount of immobilized mAb changes, the number of mAb binding sites available for interaction changes proportionally. Moreover, the ratio of the molecular masses of the reactants and the immobilized and observed response levels were used to obtain information about the activity of the surface ligand. In this work, the mass of the mAb is 75kDa per antigen binding site and the mass of monomeric PSA is 30kDa, giving a mass ratio of 0.40. The average value of the observed R_{max} vs immobilization level R_{Ab} (slope of the data in Fig. **10**) was 0.175. The difference between the observed response and the expected response based on the mass ratio was 0.4375 (i.e., maximum binding ratio). This suggested that the mAb surface was only 44% active for PSA binding.

9. CONCLUSION

The SPR techniques can be used at two levels of biomolecular interaction analysis. Firstly, in providing simple yes/no answers to the question: Does Ag bind to Ab? Secondly, they can, with care, provide accurate binding affinity and stoichiometry data. Both methods are sensitive to the binding of mass to an activated optical sensor chip surface. The literatures surveyed in this review demonstrate that SPR can successfully detect and quantitate binding of small molecule of hapten to Ab by three different interaction modes: nonequivalent two-site interaction, multiple equivalent-site interaction and multisite interaction modes. A variety of SPR approaches have been devised as described in this review for obtaining an estimate of the binding constant of an Ab for its Ag. Many immunochemical procedures involve multivalent interactions. Antibodies are multivalent; IgGs and most IgAs are bivalent, and IgMs are decavalent. Antigens can be multivalent either because they contain multiple copies of the same epitope, or because they contain multiple epitopes recognized by different Abs. It is not always easy to predict the effects of multivalency, as the reactions involve geometric arrangements that impose steric constraints. However, the effects of multivalency can be simplified by the use of SPR by considering several simple modes with a 1:1 or 1:2 stoichiometry. On the other hand, SPR has been used to evaluate the intrinsic affinities and rate constants for binding of the Ag molecules to Ab. However, to date there is no proof of concept that SPR sensing can be performed for defining exactly how many subpopulations of different affinity exist in a polyclonal Ab which contains a heterogeneous population of Abs of different affinity for the immunogen. Nevertheless, SPR sensing is emerging as a method of great value for the measurement of binding constant, dissociation rate constant and stoichiometry for Ab-Ag interaction kinetics in the emerging fields of genomics, proteomics and metabolomics.

ABBREVIATIONS

Ag	=	Antigen
BSA	=	Bovine serum albumin
DHP	=	Dihydroprogesterone
Fab	=	Antigen-binding fragment
HEL	=	Hen egg white lysozyme
K_A	=	Association constant
k_a	=	Association rate constant
K_D	=	Dissociation constant
k_d	=	Dissociation rate constant
mAb	=	Monoclonal antibody
NP	=	(4-hydroxy-3-nitrophenyl)acetyl
OVA	=	Ovalbumin
PSA	=	Prostate-specific antigen
R	=	SPR response signal
RU	=	Resonance unit
scFv	=	Variable single-chain fragment
SPR	=	Surface plasmon resonance

REFERENCES

Beernink, P. T., Hwang, M., Ramirez, M., Murphy, M. B., Doyle, S. A. and Thelen, M. P. (2005) Specificity of protein interactions mediated by BRCT domains of the XRCC1 DNA repair protein. *J. Biol. Chem.* **280**: 30206-13.

Berzofsky, J. A. and Berkower, I. J. (1983) *in*: W.E. Paul (Ed.) Antibody-antigen interaction. CRC Press, Boca Raton, FL., pp. 595-644.

Biemann, H. P. and Koshland, D. E. (1994) The proteinase: mucus proteinase inhibitor binding stoichiometry. *J. Biol. Chem.* **267**: 4370-5.

Biorn, A. C., Cocklin, S., Madani, N., Si, Z., Ivanovic, T., Samanen, J., Ryk, D. I. V., Pantophlet, R., *et al.* (2004) Model of action for linear peptide inhibitors of HIV-1 gp120 interactions. *Biochemistry* **43**: 1928-38.

Boghaert, E. R., Sridharan, L., Armellino, D. C., Khandke, K. M., DiJoseph, J. F., Kunz, A., Dougher, M. M., Jiang, F., *et al.* (2004) Antibody-targeted chemotherapy with the calicheamicin conjugate hu3S193-N-acetyl g calicheamicin dimethyl hydrazide targets Lewis and eliminates Lewis-positive human carcinoma cells and xenografts. *Clin. Cancer Res.* **10**: 4538-49.

Canziani, G. A., Klakamp, S. and Myszka, D. G. (2004) Kinetics screening of antibodies from crude hybridoma samples using Biacore. *Anal. Biochem.* **325**: 301-7.

Carrasco, C., Facompré, M., Chisholm, J. D., Vranken, D. L. V., Wilson, W. D. and Bailly, C. (2002) *Nucleic Acids Res.* **30**: 1774-81.

Chaudhury, C., Brooks, C. L., Carter, D. C., Robinson, J. M. and Anderson, C. L. (2006) Albumin binding to FcRn: Distinct from the FcRn-IgG interaction. *Biochemistry* **45**: 4983-90.

Davies, J. (1994) Review:Surface plasmon resonance-The technique and its applications to biomaterial processes. *Nanobiology* **3**: 5-16.

Djavadi-Ohaniance, L. and Friguet, B. (1992) The immunochemistry of solid-phase immunoassay. CRC Press, Boca Raton, FL, pp. 201-6.

Drake, A. W., Myszka, D. G. and Klakamp, S. L. (2004) Characterizing high-affinity antigen/antibody complexes by kinetic- and equilibrium-based methods. *Anal. Biochem.* **328**: 35-43.

Dubreuil, O., Bossus, M., Graille, M., Bilous, M., Savatier, A., Jolivet, M., Ménez, A., Stura, E., *et al.* (2005) Fine tuning of the specificity of an anti-progesterone antibody by first and second sphere residue engineering. *J. Biol. Chem.* **280**: 24880-7.

Fountoulakis, M., Zulauf, M., Lustig, A. and Garotta, G. (1992) Stoichiometry of interaction between interferon gamma and its receptor. *Eur. J. Biochem.* **208**: 781-7.

Glaser, R.W. (1993) Antigen-antibody binding and mass transport by convection and diffusion to a surface: a two-dimensional computer model of binding and dissociation kinetics. *Anal. Biochem.* **213**: 152-61.

Goldberg, M. (1991) Investigating protein conformation, dynamics and folding with monoclonal antibodies. *TIBS* **16**: 358-62.

Gomes, P. and Andreu, D. (2002) Direct kinetic assay of interactions between small peptides and immobilized antibodies using a surface plasmon resonance biosensor. *J. Immunol. Methods* **259**: 217-30.

Herr, A. B., White, C. L., Milburn, C., Wu, C. and Bjorkman, P. J. (2003) Bivalent binding of IgA1 to FcaRI suggests a mechanism for cytokine activation of IgA phagocytosis. *J. Mol. Biol.* **327**: 645-57.

Huang, B. C., Davern, S. and Kennel, S. J. (2006) Mono and bivalent binding of scFv and covalent diabody to murine laminin-1 using radioiodinated proteins and SPR measurements: effects on tissue retention *in vivo*. *J. Immunol. Methods* **313**: 149-60.

Ja, W. W., Olsen, B. N. and Roberts, R. W. (2005) Epitope mapping using mRNA display and a unidirectional nested deletion library. *Protein Eng. Des. Sel.* **18**: 309-19.

Johansson, R., Ohlin, M., Jansson, B. and Ohlson, S. (2006) Transiently binding antibody fragments against Lewis x and sialyl-Lewis x. *J. Immunol. Methods* **312**: 20-6.

Jonsson, U. (1992) Real time BIA. A new biosensor based technology for the direct measurement of biomolecular interactions. *Biosensors:* Fundamentals, Technologies and Applications. Ed. Scheller F. and Schmid R. D., pp. 467-476.

Katsamba, P. S., Navratilova, I., Calderon-Cacia, M., Fan, L., Thornton, K., Zhu, M., Bos, T. V., Forte, C., *et al.* (2006) Kinetic analysis of a high-affinity antibody/antigen interaction performed by multiple Biacore users. *Anal. Biochem.* **352**: 208-21.

Lackmann, M., Bucci, T., Mann, R. J., Kravets, L. A., Viney, E., Smith, F., Moritz, R. L., Carter, W., *et al.* (1996) Purification of a ligand for the EPH-like receptor HEK using a biosensor-based affinity detection approach. *Proc. Natl. Acad. Sci. USA* **93**: 2523-7.

Leickt, L., Grubb, A. and Ohlson, S. (2002) Development of monoclonal antibodies against creatine kinase MB2. *Scand J. Clin. Lab. Invest.* **62**: 423-30.

Lin, L.-P., Huang, L.-S., Lin, C.-W., Lee, C.-K., Chen, J.-L., Hsu, S.-M. and Lin, S. (2005) Determination of binding constant of DNA-binding drug to target DNA by surface plasmon resonance biosensor technology. *Curr. Drug Targets* **5**: 61-72.

Liu, X., Wei, J., Song, D., Zhang, Z., Zhang, H. and Luo, G. (2003) Determination of affinities and antigenic epitopes of bovine cardiac troponin I (cTnI) with monoclonal antibodies by surface plasmon resonance biosensor. *Anal. Biochem.* **314**: 301-9.

Liu, Z., Li, F. and Huang, Y. (1999) Determination of unbound drug concentration and protein-drug binding fraction in plasma. *Biomed. Chromatogr.* **13**: 262–6.

Ma, Q., Shimaoka, M., Lu, C., Jing, H., Carman, C. V. and Springer, T. A. (2002) Activation-induced conformational changes in the I domain region of lymphocyte function-associated antigen 1. *J. Biol. Chem.* **277**: 10638-41.

Markey, F. (1999) What is SPR anyway? *BIA. J.* **6**: 14-7.

Markgren, P.-O., Hämäläinen, M. and Danielson, U. (1999) Screening of compounds interacting with HIV-1 proteinase using optical biosensor technology. *Anal. Biochem.* **265**: 340-50.

Mazur, S., Tanious, F. A., Ding, D., Kumar, A., Boykin, D. W., Simpson, I. J., Neidle, S. and Wilson, W. D. (2000) A thermodynamic and structural analysis of DNA minor-groove complex formation. *J. Mol. Biol.* **300**: 321-37.

Mimura, Y., Sondermann, P., Ghirlando, R., Lund, J., Young, S. P., Goodall, M. and Jefferis, R. (2001) Role of oligosaccharide residues of IgG1-Fc in FccRIIb binding. *J. Biol. Chem.* **276**: 45539-45547.

Morton, T. A. and Myszka, D. G. (1998) Kinetic analysis of macromolecular interactions using surface plasmon resonance biosensors. *Methods Enzymol.* **295**: 268-94.

Myszka, D. G. (1999) Survey of the 1998 optical biosensor literature. *J. Mol. Recognit.* **12**: 390-408.

Myszka, D. G., Jonsen, M. D. and Graves, B. J. (1998) Equilibrium analysis of high affinity interactions using BIACORE. *Anal. Biochem.* **265**: 326-30.

Nguyen, B., Tardy, C., Bailly, C., Colson, P., Houssier, C., Kumar, A., Boykin, D. W. and Wilson, W. D. (2002) Influence of compound structure on affinity, sequence selectivity, and mode of binding to DNA for unfused aromatic dications related to furamidine. *Biopolymers* **63**: 281-97.

Oda, M. and Azuma T. (2000) Reevaluation of stoichiometry and affinity/avidity in interactions between anti-hapten antibodies and mono- or multi-valent antigens. *Mol. Immunol.* **37**: 1111-22.

Oda, M., Uchiyama, S., Robinson, C. V., Fukui, K., Kobayashi, Y. and Azuma, T. (2006) Regional and segmental flexibility of antibodies in interaction with antigens of different size. *FEBS J.* **273**: 1476-87.

Okun, V. M., Moser, R., Blaas, D. and Kenndler, E. (2001) Complexes between monoclonal antibodies and receptor fragments with a common cold virus: determination of stoichiometry by capillary electrophoresis. *Anal. Chem.* **73**: 3900-6.

Paetz, A., Sack, M., Thepen, T., Tur, M. K., Bruell, D., Finnern, R., Fischer, R. and Barth, S. (2005) Recombinant soluble human Fcg receptor I with picomolar affinity for immunoglobulin G. *Biochem. Biophys. Res. Commun.* **338**: 1811-7.

Ricard-Blum, S., Bernocco, S., Font, B., Moali, C. Eichenberger, D., Farjane, J., Burchardt, E. R., van der Rest, M., *et al.* (2002) Interaction properties of the procollagen C-proteinase enhancer protein shed light on the mechanism of stimulation of BMP-1. *J. Biol. Chem.* **277**: 33864-9.

Rich, R. L. and Myszka, D. G. (2000) Advances in surface plasmon resonance biosensor analysis. *Curr. Opin. Biotech.* **11**: 54-61.

Roos, H., Karlsson, R., Nilshans, H. and Persson, A. (1998) Thermodynamic analysis of protein interactions with biosensor technology. *J. Mol. Recognit.* **11**: 204-10.

Russo, K., Ragone, R., Facchiano, A. M., Capogrossi, M. C. and Facchiano, A. (2002) Platelet-derived growth factor-BB abd basic fibroblast growth factor directly interact *in vitro* with high affinity. *J. Biol. Chem.* **277**: 1284-91.

Sagawa, T., Oda, M., Ishimura, M., Furukawa, K. and Azuma, T. (2003) Thermodynamic and kinetic aspects of antibody evolution during the immune response to hapten. *Mol. Immunol.* **39**: 801-8.

Son, J. H., Lee, U. H., Lee, J. J., Kwon, B., Kwon, B. S. and Park, J. W. (2004) Humanization of agonistic anti-human 4-1BB monoclonal antibody using a phag-displayed combinatorial library. *J. Immunol. Methods* **286**: 187-201.

Teulade-Fichou, M. P., Carrasco, C., Guittat, L., Bailly, C., Alberti, P., Mergny, J. L., David, A., Lehn, J. M., *et al.* (2003) Selective recognition of G-qQuadruplex telomeric DNA by a bis(quinacridine) macrocycle. *J. Am. Chem. Soc.* **125**: 4732-40.

Tobita, T., Oda, M. and Azuma, T. (2004) Segmental flexibility and avidity of IgM in the interaction of polyvalent antigens. *Mol. Immunol.* **40**: 803-11.

Verel, I., Heider, K. H., Siegmund, M., Ostermann, E., Patzelt, E., Sproll, M., Snow, G. B., Adolf, G. R., *et al.* (2002) Tumor targeting properties of monoclonal antibodies with different affinity for target antigen

CD44V6 in nude mice bearing head-and-neck cancer xenografts. *Int. J. Cancer* **99**: 396-402.

Wittel, U. A., Jain, M., Goel, A., Baranowska-Kortylewicz, J., Kurizaki, T., Chauhan, S. C., Agrawal, D. K., Colcher, D., *et al.* (2005) Engineering and characterization of a divalent single-chain Fv angiotensin II fusion contruct of the monoclonal antibody CC49. *Biochem. Biophys. Res. Commun.* **329**: 168-76.

Yang, C. Y., Brooks, E., Li, Y., Denny, P., Ho, C. M., Qi, F., Shi, W., Wolinsky, L., *et al.* (2005) Detection of picomolar levels of interleukin-8 in human saliva by SPR. *Lab Chip* **5**: 1017-23.

Zeder-Lutz, G., Neurath, A. R. and Van Regenmortel, M. H. (1999) Kinetics of interaction between 3-hydroxyphthaloyl-beta-lactoglobulin and CD4 molecules. *Biologicals* **27**: 29-34.